We are IntechOpen, the world's leading publisher of Open Access books Built by scientists, for scientists

4,800
Open access books available

122,000
International authors and editors

135M
Downloads

Our authors are among the

154
Countries delivered to

TOP 1%
most cited scientists

12.2%
Contributors from top 500 universities

CLARIVATE ANALYTICS BOOK CITATION INDEX INDEXED

WEB OF SCIENCE™

Selection of our books indexed in the Book Citation Index in Web of Science™ Core Collection (BKCI)

Interested in publishing with us?
Contact book.department@intechopen.com

Numbers displayed above are based on latest data collected.
For more information visit www.intechopen.com

10

Stereo Measurement of Objects in Liquid and Estimation of Refractive Index of Liquid by Using Images of Water Surface

Atsushi Yamashita, Akira Fujii and Toru Kaneko
Shizuoka University
Japan

1. Introduction

In this paper, we propose a new stereo measurement method of objects in liquid whose refractive index is unknown.
In recent years, demands for underwater tasks, such as digging of ocean bottom resources, exploration of aquatic environments, rescues, and salvages, have increased. Therefore, underwater robots or underwater sensing systems that work instead of human become important, and technologies for observing underwater situations correctly and robustly from cameras of these systems are needed (Yuh, 2001). However, it is very difficult to observe underwater environments with cameras (Hulburt, 1945; Stewart, 1991; Caimi, 1996), because of the following three big problems.

1. View-disturbing noise (Fig. 1(a))
2. Light attenuation effect (Fig. 1(b))
3. Light refraction effect (Fig. 1(c))

The first problem is about suspended matters, such as bubble noises, small fishes, small creatures, and so on. They may disturb camera's field of view (Fig. 1(a)).

(a) View-disturbing noise. (b) Light attenuation effect. (c) Light refraction effect.

Fig. 1. Examples of aquatic images.

The second problem is about the attenuation effects of light. The light intensity decreases with the distance from objects in water by light attenuation depending on the wavelength of light. Red light decreases easier than blue light in water (Hulburt, 1945). In this way, colors of objects observed in underwater environments are different from those in air (Fig. 1(b)).

Those two problems make it very difficult to detect or to recognize objects in water by observing their textures and colors.
As to these two problems, theories or methods for aerial environments can be expanded for underwater sensing. Several image processing techniques can be effective for removing adherent noises. Color information can be also restored by considering reflection, absorption, and scattering phenomena of light in theory (Hulburt, 1945). Indeed, we have already proposed underwater sensing methods for the view-disturbing noise problem (Yamashita et al., 2006) and the light attenuation problem (Yamashita et al., 2007).
The third problem is about the refraction effects of light. If cameras and objects are in the different condition where the refraction index differs from each other, several problems occur and a precise measurement cannot be achieved.
For example, Fig. 1(c) shows an image of a duck model when water is filled to the middle. In this case, contour positions of the duck model above and below the water surface looks discontinuous and disconnected, and its size and the shape look different between above and below the water surface. This problem occurs not only when a vision sensor is set outside the liquid but also when it is set inside, because in the latter case we should usually place a protecting glass plate in front of viewing lens.
As to the light refraction problem, three-dimensional (3-D) measurement methods in aquatic environments are also proposed (Coles, 1988; Tusting & Davis, 1992; Pessel et al., 2003; Li et al., 1997; Yamashita et al., 2010). However, techniques that do not consider the influence of the refraction effects (Coles, 1988; Tusting & Davis, 1992; Pessel et al., 2003) may have the problems of accuracy.
Accurate 3-D measurement methods of objects in liquid with a laser range finder (Yamashita et al., 2003; Yamashita et al., 2004; Kondo et al., 2004; Yamashita et al., 2005) and with a light projection method (Kawai et al., 2009) by considering the refraction effects are also proposed. However, it is difficult to measure moving objects with these methods.
A stereo camera system is suitable for measuring moving objects, though the methods by using a stereo camera system (Li et al., 1997) have the problem that the corresponding points are difficult to detect when the texture of the object's surface is simple in particular when there is the refraction on the boundary between the air and the liquid. The method by the use of motion stereo images obtained with a moving camera (Saito et al., 1995) also has the problem that the relationship between the camera and the object is difficult to estimate because the camera moves. The surface shape reconstruction method of objects by using an optical flow (Murase, 1992) is not suitable for the accurate measurement, too.
By using properly calibrated stereo systems, underwater measurements can be achieved without knowing the refraction index of the liquid. For example, we can make a calibration table of relations between distances and pixel positions in advance and utilize this table for 3-D measurement (Kondo et al., 2004). However, the calibration table is useless when the refractive index of liquid changes.
Therefore, the most critical problem in aquatic environments is that previous studies cannot execute the 3-D measurement without the information of the refractive index of liquid (Li et al., 1997; Yamashita et al., 2006). It becomes difficult to measure precise positions and shapes of objects when unknown liquid exists because of the image distortion by the light refraction.
Accordingly, it is very important to estimate the refractive index for underwater sensing tasks.

In this paper, we propose a new 3-D measurement method of objects in unknown liquid with a stereo vision system. The refractive index of unknown liquid is estimated by using images of water surface (Fig. 2). Discontinuous and disconnected edges of the object in the image of the water surface can be utilized for estimating the refractive index. A 3-D shape of the object in liquid is measured by using the estimated refractive index in consideration of refractive effects. In addition, images that are free from refractive effects of the light are restored from distorted images.

Our proposed method is easy to apply to underwater robots. If there is no information about refractive index of work space of an underwater robot, the robot can know the refractive index and then measure underwater objects only by broaching and acquiring an image of water surface.

The composition of this paper is detailed below. In Section 2, an estimation method of the refractive index is explained. In Sections 3 and 4 describe a 3-D measurement and image restoration method that are based on the ray tracing technique, respectively. Sections 5 and 6 mention about experiments and discussion. Section 7 describes conclusions.

2. Estimation of refractive index

There is the influence of the light refraction in liquid below the water surface, while there is no influence above the water surface. An image below the water surface is distorted in consequence of the light refraction effect in liquid, and that above the water surface is not distorted (Fig. 2). Therefore, such discontinuous contour indicates the refraction information. We utilize the difference between edges in air and those in liquid to estimate the refractive index of the liquid.

Figure 3 shows the top view of the situation around the water surface region when the left edge of the object is observed from the right camera.

Here, let u_1 be a horizontal distance in image coordinate between image center and the object edge in air, and u_2 be that in liquid. Note that u_1 is influenced only by the refraction effect in glass (i.e. camera protection glass), and u_2 is influenced by the refraction effects both in glass and in liquid (Lower figure in Fig. 3).

Angles of incidence from air to glass in these situations (θ_1 and θ_4) are expressed as follows:

$$\theta_1 = \phi + \tan^{-1}\frac{u_2}{f} \tag{1}$$

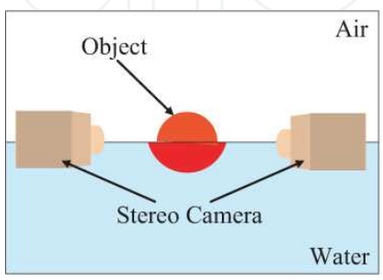

Fig. 2. Stereo measurement of objects in liquid by using images of water surface. An image below the water surface is distorted in consequence of the light refraction effect in liquid, and that above the water surface is not distorted.

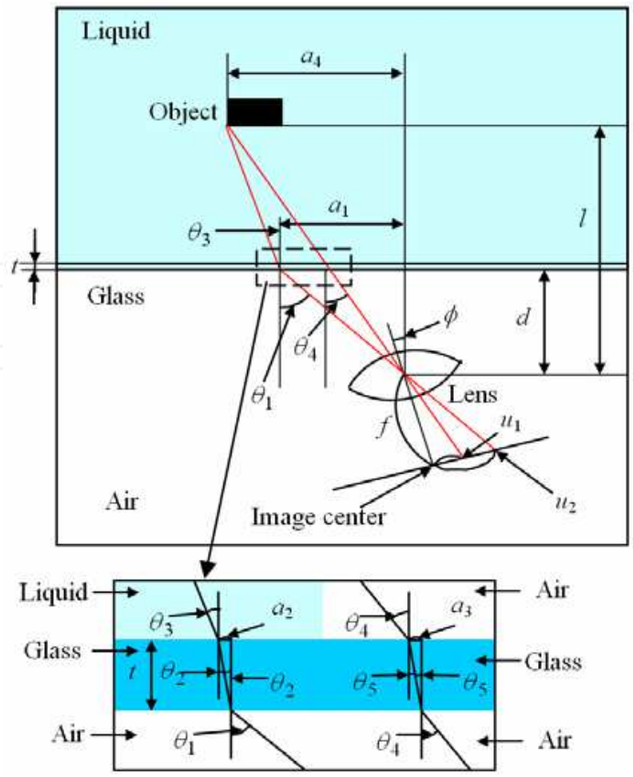

Fig. 3. Estimation of refractive index.

$$\theta_4 = \phi + \tan^{-1}\frac{u_1}{f} \tag{2}$$

where ϕ is the angle between the optical axis of the camera and the normal vector of the glass, and f is the image distance (the distance between the lens center and the image plane), respectively.

Parameters f and ϕ can be calibrated easily in advance of the measurement, and coordinate values u_1 and u_2 can be obtained from the acquired image of the water surface. Therefore, we can calculate θ_1 and θ_4 from these known parameters.

By using Snell's law of refraction, angles of refraction (θ_2 and θ_5) are expressed as follows:

$$\frac{n_1}{n_2} = \frac{\sin\theta_2}{\sin\theta_1} \tag{3}$$

$$\frac{n_1}{n_2} = \frac{\sin\theta_5}{\sin\theta_4} \tag{4}$$

where n_1 is the refractive index of air, and n_2 is that of glass, respectively.

On the other hand, we can obtain a_1, a_2, a_3, and a_4 from the geometrical relationship among the lens, the glass, and the object.

$$a_1 = d\tan\theta_1 \tag{5}$$

$$a_2 = t\tan\theta_2 \tag{6}$$

$$a_3 = t\tan\theta_5 \tag{7}$$

$$a_4 = (l-t)\tan\theta_4 + a_3 \tag{8}$$

where d is the distance between the lens center and the glass surface, t is the thickness of the glass, and l is the distance between the lens center and the object.
Refractive indices n_1 and n_2 can be calibrated beforehand because they are fixed parameters. Parameters d and t can be calibrated in advance of the measurement, too. This is because we usually placed a protecting glass in front of the lens when we use a camera in liquid, and the relationship between the glass and the lens never changes. Parameter l can be gained from the stereo measurement result of the edge in air.
By using these parameters, angle of refraction from glass to liquid θ_3 can be calculated as follow:

$$\theta_3 = \tan^{-1}\frac{a_4 - a_2 - a_1}{l - t - d} \tag{9}$$

Consequently, refractive index of liquid n_3 can be obtained by using Snell's law.

$$n_3 = n_1\frac{\sin\theta_1}{\sin\theta_3} \tag{10}$$

In this way, we can estimate refractive index of unknown liquid n_3 from the image of water surface, and measure objects in liquid by using n_3.

3. 3-D measurement

It is necessary to search for corresponding points from right and left images to measure the object by using the stereo vision system. In our method, corresponding points are searched for with template matching by using the normalized cross correlation (NCC) method.
After detecting corresponding points, an accurate 3-D measurement can be executed by considering the refraction effects of light in aquatic environments.
Refractive angles at the boundary surfaces among air, glass and liquid can be determined by using Snell's law (Fig. 4).
We assume the refractive index of air and the glass to be n_1 and n_2, respectively, and the incidence angle from air to the glass to be θ_1. A unit ray vector $\vec{d}_2 = (\alpha_2, \beta_2, \gamma_2)^T$ (T denotes transposition) travelling in the glass is shown by (11).

$$\begin{pmatrix}\alpha_2\\ \beta_2\\ \gamma_2\end{pmatrix} = \frac{n_1}{n_2}\begin{pmatrix}\alpha_1\\ \beta_1\\ \gamma_1\end{pmatrix} + \left(\sqrt{1-\frac{n_1^2}{n_2^2}\sin^2\theta_1} - \frac{n_1}{n_2}\cos\theta_1\right)\begin{pmatrix}\lambda\\ \mu\\ \nu\end{pmatrix} \tag{11}$$

where $\vec{d}_1 = (\alpha_1, \beta_1, \gamma_1)^T$ is the unit ray vector of the camera in air and $\vec{N} = (\lambda, \mu, \nu)^T$ is a normal vector of the glass plane. Vector $\vec{d}_1$ can be easily calculated from the coordinate value of the corresponding point, and vector $\vec{N}$ can be calibrated in advance of the measurement as described above.

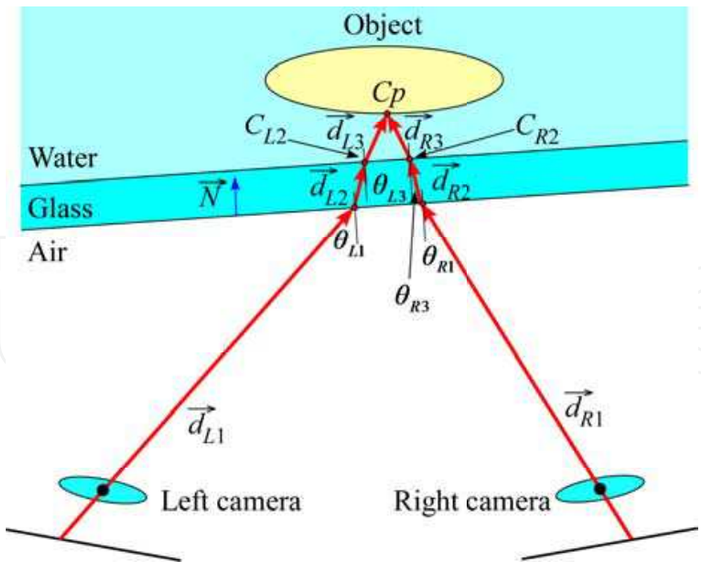

Fig. 4. 3-D measurement.

A unit ray vector $\vec{d}_3 = (\alpha_3, \beta_3, \gamma_3)^T$ travelling in liquid is shown by (12).

$$\begin{pmatrix} \alpha_3 \\ \beta_3 \\ \gamma_3 \end{pmatrix} = \frac{n_2}{n_3} \begin{pmatrix} \alpha_2 \\ \beta_2 \\ \gamma_2 \end{pmatrix} + \left(\sqrt{1 - \frac{n_2^2}{n_3^2} \sin^2 \theta_3} - \frac{n_2}{n_3} \cos \theta_3 \right) \begin{pmatrix} \lambda \\ \mu \\ \nu \end{pmatrix} \tag{12}$$

where n_3 is the refractive index of liquid that is estimated in Section 2, and θ_3 is the angle of incidence from the glass to liquid, respectively.

An arbitrary point $\vec{C}_p = (x_p, y_p, z_p)^T$ on the ray vector is shown by (13).

$$\begin{pmatrix} x_p \\ y_p \\ z_p \end{pmatrix} = c \begin{pmatrix} \alpha_3 \\ \beta_3 \\ \gamma_3 \end{pmatrix} + \begin{pmatrix} x_2 \\ y_2 \\ z_2 \end{pmatrix} \tag{13}$$

where $\vec{C}_2 = (x_2, y_2, z_2)^T$ is the point on the glass and c is a constant.

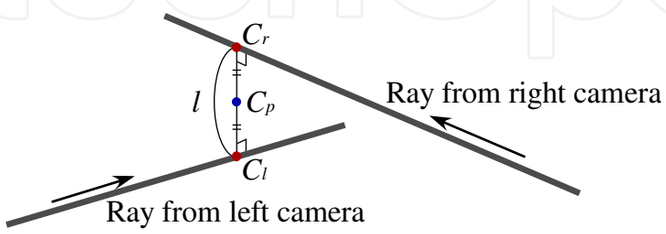

Fig. 5. Ray tracing from two cameras.

Two rays are calculated by ray tracing from the left and the right cameras, and the intersection of the two rays gives the 3-D coordinates of the target point in liquid. Theoretically, the two rays intersect at one point on the object surface, however, practically it is not always true

because of noises and quantization artifacts. Consequently, we select the midpoint of the shortest line connecting two points each of which belongs to each ray (Fig. 5).
Note that the detail of the solution is explained in (Yamashita et al., 2003).

4. Image restoration

Images that are free from the refraction effects can be generated from distorted images by using 3-D information acquired in Section 3.
Figure 6 shows the top view of the situation around the water surface region. Here, let e_2 be the image coordinate value that is influenced by the refraction effect in liquid, and e_1 be the image coordinate value that is rectified (in other word, free from the refraction effect of liquid). The purpose is to reconstruct a new image by obtaining e_1 from the observed value e_2.
In Fig. 6, the image distance (f), the angle between the optical axis of the camera and the normal vector of the glass (ϕ), the distance between the lens center and the glass (d), the thickness of the glass (t), the distance between the image center and e_2 (g_{2x}), and the distance between the lens and the object (z_i) is known parameters.
We can restore the image if g_{1x} (the distance between the image center and e_1) is obtained.
At first, angle of incidence θ_{1x} is expressed as follows:

$$\theta_{1x} = \phi + \tan^{-1}\frac{g_{2x}}{f} \tag{14}$$

Angle of refraction from air to glass θ_{2x} and that from glass to liquid θ_{3x} is obtained by using Snell's law.

$$\theta_{2x} = \sin^{-1}\frac{n_1 \sin\theta_{1x}}{n_2} \tag{15}$$

$$\theta_{3x} = \sin^{-1}\frac{n_1 \sin\theta_{1x}}{n_3} \tag{16}$$

On the other hand, parameters a_{1x}, a_{2x}, and a_{3x} are obtained from the geometrical relationship in Fig. 6.

$$a_{1x} = d\tan\theta_{1x} \tag{17}$$

$$a_{2x} = t\tan\theta_{2x} \tag{18}$$

$$a_{3x} = (z_i - t - d)\tan\theta_{3x} + a_{1x} + a_{2x} \tag{19}$$

At the same time, a_{3x} can be expressed as follows:

$$a_{3x} = (z_i - t)\tan\theta_{4x} + t\tan\theta_{5x} \tag{20}$$

Finally, we can obtain the following equation.

$$a_{3x} = (z_i - t)\tan\theta_{4x} + t\tan\left(\sin^{-1}\frac{n_1 \sin\theta_{4x}}{n_2}\right) \tag{21}$$

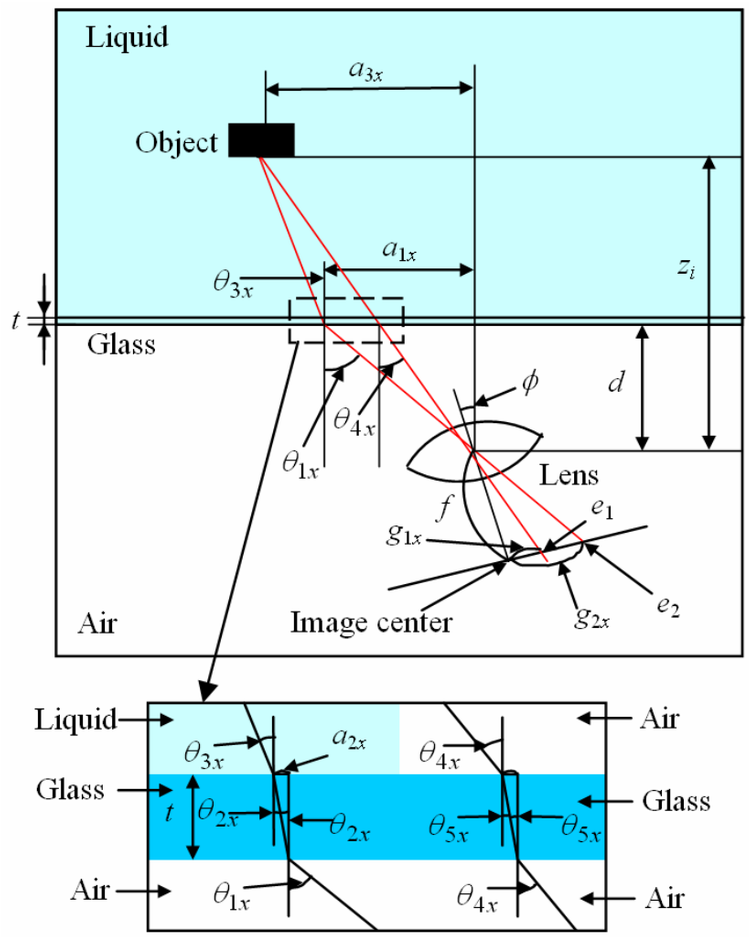

Fig. 6. Image restoration.

From (21), we can calculate θ_{4x} by numerical way. Therefore, parameter g_{1x} is gained by using obtained θ_{4x} and f.

$$g_{1x} = f \tan\theta_{4x} \tag{22}$$

By using g_{1x}, the image that is free from the refraction effect can be restored.
The vertical coordinate value after the restoration is also calculated in the same way. In this way, the image restoration is executed.
However, there may be no texture information around or on the water surface because a dark line appears on the water surface in images.
Therefore, textures of these regions are interpolated by image inpainting algorithm (Bertalmio et al., 2000). This method can correct the noise of an image in consideration of slopes of image intensities, and the merit of this algorithm is the fine reproducibility for edges.
Finally, we can obtain the restored image both below and around the water surface.

5. Experiment

We constructed an underwater environment by using a water tank (Fig. 7). It is an equivalent optical system to sinking the waterproof camera in underwater. We used two digital video cameras for taking images whose sizes are 720x480pixels. We set the optical axis parallel to the plane of the water surface.

In the experiment, the geometrical relationship between two cameras and the glass, the thickness of the glass, and intrinsic camera parameters (Tsai, 1987) were calibrated before the 3-D measurement in air. These parameters never change regardless of whether there is water or not.

To evaluate the validity of the proposed method, two objects are measured in liquid whose refractive index is unknown. Object 1 is a duck model and Object 2 is a cube.

Object 1 (duck model) floated on the water surface, and Object 2 (cube) was put inside the liquid (Fig. 7).

Figures 8(a) and (b) show acquired left and right images of the water surface, respectively.

At first, the refractive index of unknown liquid (n_3) is estimated from four edge positions inside red circles. Table 1 shows the result of estimation. The variation of the results is small enough to trust, and the average of four results is 1.333, while the ground truth is 1.33 because we used water as unknown liquid.

From this result, it is verified that our method can estimate the refractive index precisely.

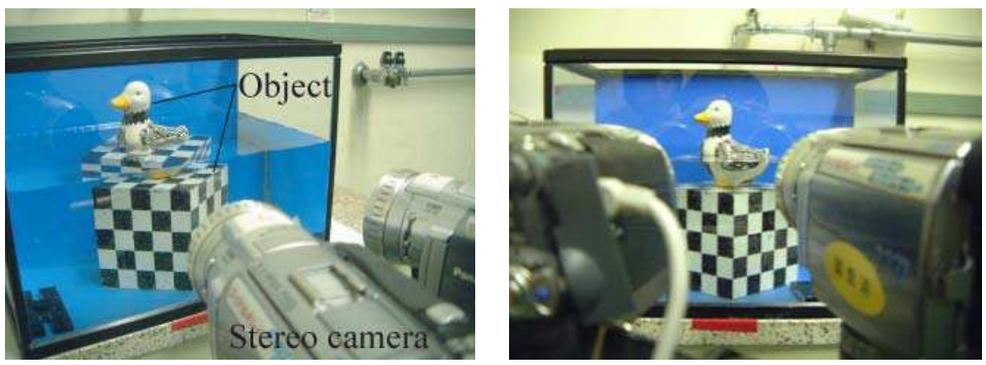

(a) Birds-eye view. (b) Front view.

Fig. 7. Overview of experiments.

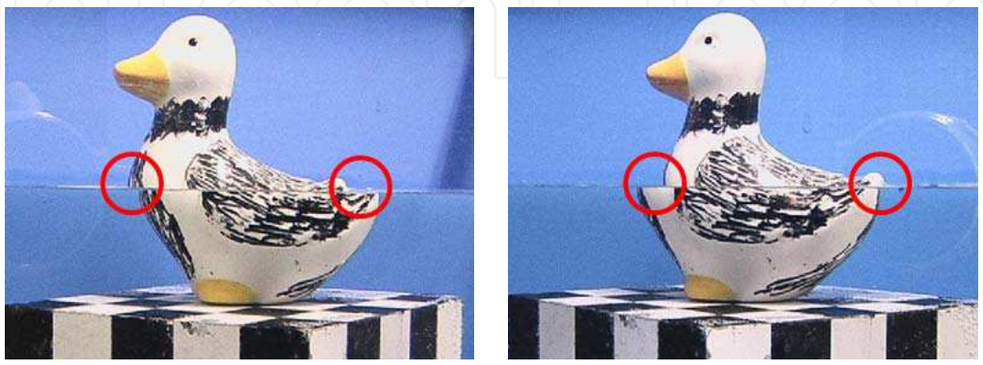

(a) Left image. (b) Right image.

Fig. 8. Stereo image pair.

Left camera		Right camera		Average
Left edge	Right edge	Left edge	Right edge	
1.363	1.335	1.334	1.300	1.333

Table 1. Estimation result of refractive index.

Figure 9 shows the 3-D shape measurement result of Object 1. Figure 9(a) shows the result without consideration of light refraction effect. There is the disconnection of 3-D shape between above and below the water surface. Figure 9(b) shows the result by our method. Continuous shape can be acquired, although the acquired images have discontinuous contours (Fig. 8).

By using the estimated refractive index, the shape of Object 2 (cube) was measured quantitatively. When the refractive index was unknown (n_3 = 1.000) and the refraction effect was not considered, the vertex angle was measured as 111.1deg, while the ground truth was 90.0deg. On the other hand, the result was 90.9deg when the refraction effect was considered by using the estimated refractive index.

From these results, it is verified that our method can measure accurate shape of underwater objects.

Figure 10 shows the result of the image restoration. Figure 10(a) shows the original image, Fig. 10(b) shows extracted result of the object by using color extraction method (Smith et al., 1996), and Fig. 10(c) shows the restoration result, respectively.

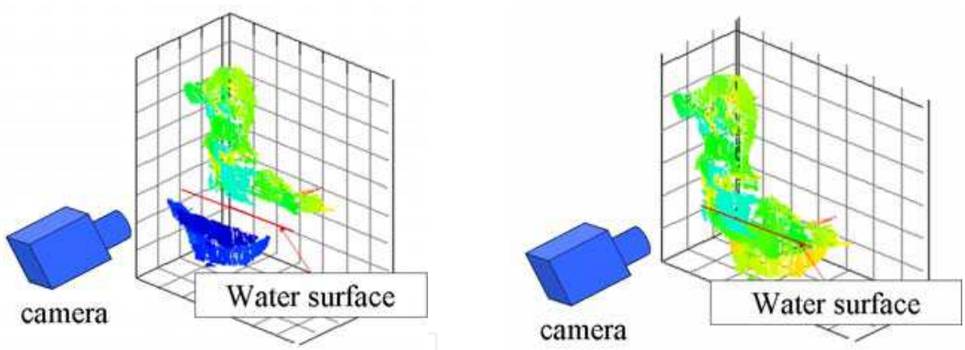

(a) Without consideration. (b) With consideration.

Fig. 9. 3-D measurement results.

(a) Original image. (b) Extraction result. (c) Image restoration result.

Fig. 10. Image restoration results.

These results show that our method can work well without failure regardless of the existence of unknown liquid by estimating the refractive index of liquid and considering the light refraction.

6. Discussion

As to the estimation of the refractive index, the error of the estimation is within 1% through all experiments.

The accuracy and the stability is very high, however, the proposed method needs image pairs of the water surface. Therefore, this method may not be applicable directly for deep water applications, because the refractive index changes little by little when water pressure and temperature change. On the other hand, we can use the distance between two rays (l in Fig. 5) for the estimation when water surface images are difficult to obtain. The value of the refractive index in case that the distance between two rays becomes the smallest is a correct one. Therefore, the refractive index n_{est} can be estimated by using following optimization.

$$n_{est} = \arg\min_{n} \sum_{i} l_i(n) \tag{23}$$

where $l_i(n)$ is the calculated distance between two rays at i-th measurement point when the refractive index is presumed as n. However, this method is not robust because it is very sensitive to an initial value of the estimation. Therefore, it is better to use both two approaches for deep water applications; at first in shallow water the refractive index is estimated by using water surface images, then in deep water by using the distance between two rays.

As to the refraction effects, they may be reduced by using an individual spherical protective dome for each camera. However, it is impossible to eliminate the refraction effects. Therefore, our method is essential to the precise measurement in underwater environments.

As to the image restoration, near the water surface appears an area without information in form of a black strip. We cannot have information about this area. Therefore, textures of these regions are interpolated for visibility. Note that 3-D measurement explained in Section 3 can be achieved without the image restoration. Therefore, 3-D measurement results do not include interpolated results. This means that the proposed method shows both reliable results that is suitable for underwater recognition and images that have good visibility for the sake of human operators.

	With consideration	Without consideration
Average	2.0mm	36.1mm
Standard deviation	0.4mm	1.1mm

Table 2. Accuracy of measurement (position error).

To evaluate the proposed method quantitatively, another well-calibrated objects whose shapes are known and whose positions were measured precisely in air in advance were measured in water. Table 2 shows the measurement result. In this experiment, mis-corresponding points were rejected by a human operator. Position error with

consideration of the refraction effects is 2.0mm on an average when the distance between the stereo camera system and the object is 250mm, while the error without consideration of the refraction effects is 36.1mm. The error in the depth direction was dominant in all cases.
From these results, it is verified that our method can measure accurate positions of objects in water.

7. Conclusion

We propose a 3-D measurement method of objects in unknown liquid with a stereo vision system. We estimate refractive index of unknown liquid by using images of water surface, restore images that are free from refractive effects of the light, and measure 3-D shapes of objects in liquids in consideration of refractive effects. The effectiveness of the proposed method is verified through experiments.
It is expected that underwater robots acquire the refractive index and then measure underwater objects only by broaching and acquiring an image of water surface in the case of unknown refractive index by using our method.

8. Acknowledgement

This research was in part supported by MEXT KAKENHI, Grant-in-Aid for Young Scientist (A), 22680017.

9. References

Yuh, J. & West, M. (2001). Underwater Robotics, *Advanced Robotics*, Vol.15, No.5, pp.609-639

Hulburt, E. O. (1945). Optics of Distilled and Natural Water, *Journal of the Optical Society of America*, Vol.35, pp.689-705

Stewart, W. K. (1991). Remote-Sensing Issues for Intelligent Underwater Systems, *Proceedings of the 1991 IEEE Computer Society Conference on Computer Vision and Pattern Recognition (CVPR1991)*, pp.230-235

Caimi, F. M. (1996). Selected Papers on Underwater Optics, *SIPE Milestone Series*, Caimi, F. M. (Ed.), Vol.MS118

Yamashita, A.; Kato, S. & Kaneko, T. (2006). Robust Sensing against Bubble Noises in Aquatic Environments with a Stereo Vision System, *Proceedings of the 2006 IEEE International Conference on Robotics and Automation (ICRA2006)*, pp. 928-933

Yamashita, A.; Fujii, M. & Kaneko, T. (2007). Color Registration of Underwater Images for Underwater Sensing with Consideration of Light Attenuation, *Proceedings of the 2007 IEEE International Conference on Robotics and Automation (ICRA2007)*, pp.4570-4575

Coles, B. W. (1988). Recent Developments in Underwater Laser Scanning Systems, *SPIE Vol.980 Underwater Imaging*, pp.42-52

Tusting, R. F. & Davis, D. L. (1992). Laser Systems and Structured Illumination for Quantitative Undersea Imaging, *Marine Technology Society Journal*, Vol.26, No.4, pp.5-12

Pessel, N.; Opderbecke, J. & Aldon, M.-J. (2003). Camera Self-Calibration in Underwater Environment, *Proceedings of the 11th International Conference in Central Europe on Computer Graphics, Visualization and Computer Vision (WSCG2003)*, pp.104-110

Li, R.; Li, H.; Zou, W.; Smith, R. G. & Curran, T. A. (1997). Quantitive Photogrammetric Analysis of Digital Underwater Video Imagery, *IEEE Journal of Oceanic Engineering*, Vol.22, No.2, pp.364-375

Yamashita, A.; Shirane, Y. & Kaneko, T. (2010). Monocular Underwater Stereo - 3D Measurement Using Difference of Appearance Depending on Optical Paths -, *Proceedings of the 2010 IEEE/RSJ International Conference on Intelligent Robots and Systems (IROS2010)*

Yamashita, A.; Hayashimoto, E.; Kaneko, T. & Kawata, Y. (2003). 3-D Measurement of Objects in a Cylindrical Glass Water Tank with a Laser Range Finder, *Proceedings of the 2003 IEEE/RSJ International Conference on Intelligent Robots and Systems (IROS2003)*, pp.1578-1583

Yamashita, A.; Higuchi, H.; Kaneko, T. & Kawata, Y. (2004). Three Dimensional Measurement of Object's Surface in Water Using the Light Stripe Projection Method, *Proceedings of the 2004 IEEE International Conference on Robotics and Automation} (ICRA2004)*, pp.2736-2741

Kondo, H.; Maki, T.; Ura, T.; Nose, Y.; Sakamaki, T. & Inaishi, M. (2004). Relative Navigation of an Autonomous Underwater Vehicle Using a Light-Section Profiling System, *Proceedings of the 2004 IEEE/RSJ International Conference on Intelligent Robots and Systems (IROS2004)*, pp.1103-1108

Yamashita, A.; Ikeda, S. & Kaneko, T. (2005). 3-D Measurement of Objects in Unknown Aquatic Environments with a Laser Range Finder, *Proceedings of the 2005 IEEE International Conference on Robotics and Automation (ICRA2005)*, pp. 3923-3928

Kawai, R.; Yamashita, A. & Kaneko, T. (2009). Three-Dimensional Measurement of Objects in Water by Using Space Encoding Method, *Proceedings of the 2009 IEEE International Conference on Robotics and Automation (ICRA2009)*, pp.2830-2835

Saito, H.; Kawamura, H. & Nakajima, M. (1995). 3D Shape Measurement of Underwater Objects Using Motion Stereo, *Proceedings of 21th International Conference on Industrial Electronics, Control, and Instrumentation*, pp.1231-1235

Murase, H. (1992). Surface Shape Reconstruction of a Nonrigid Transparent Object Using Refraction and Motion, *IEEE Transactions on Pattern Analysis and Machine Intelligence*, Vol.14, No.10, pp.1045-1052

Bertalmio, M.; Sapiro, G.; Caselles, V. & Ballester, C. (2000). Image Inpainting, *ACM Transactions on Computer Graphics (Proceedings of SIGGRAPH2000)*, pp.417-424

Tsai, R. Y. (1987). A Versatile Camera Calibration Technique for High-Accuracy 3D Machine Vision Metrology Using Off-the-Shelf TV Cameras and Lenses, *IEEE Journal of Robotics and Automation*, Vol.RA-3, No.4, pp.323-344

Smith, A. R. & Blinn, J. F. (1996). Blue Screen Matting, *ACM Transactions on Computer Graphics (Proceedings of SIGGRAPH1996)*, pp.259-268

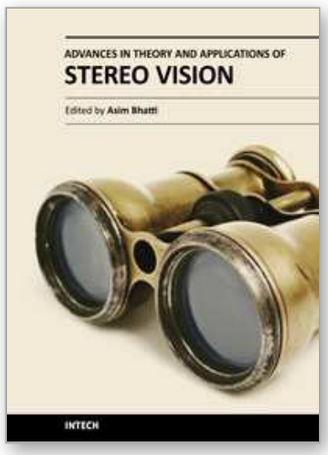

Advances in Theory and Applications of Stereo Vision
Edited by Dr Asim Bhatti

ISBN 978-953-307-516-7
Hard cover, 352 pages
Publisher InTech
Published online 08, January, 2011
Published in print edition January, 2011

The book presents a wide range of innovative research ideas and current trends in stereo vision. The topics covered in this book encapsulate research trends from fundamental theoretical aspects of robust stereo correspondence estimation to the establishment of novel and robust algorithms as well as applications in a wide range of disciplines. Particularly interesting theoretical trends presented in this book involve the exploitation of the evolutionary approach, wavelets and multiwavelet theories, Markov random fields and fuzzy sets in addressing the correspondence estimation problem. Novel algorithms utilizing inspiration from biological systems (such as the silicon retina imager and fish eye) and nature (through the exploitation of the refractive index of liquids) make this book an interesting compilation of current research ideas.

How to reference
In order to correctly reference this scholarly work, feel free to copy and paste the following:

Atsushi Yamashita, Akira Fujii and Toru Kaneko (2011). Stereo Measurement of Objects in Liquid and Estimation of Refractive Index of Liquid by Using Images of Water Surface, Advances in Theory and Applications of Stereo Vision, Dr Asim Bhatti (Ed.), ISBN: 978-953-307-516-7, InTech, Available from: http://www.intechopen.com/books/advances-in-theory-and-applications-of-stereo-vision/stereo-measurement-of-objects-in-liquid-and-estimation-of-refractive-index-of-liquid-by-using-images

INTECH
open science | open minds

InTech Europe
University Campus STeP Ri
Slavka Krautzeka 83/A
51000 Rijeka, Croatia
Phone: +385 (51) 770 447
Fax: +385 (51) 686 166
www.intechopen.com

InTech China
Unit 405, Office Block, Hotel Equatorial Shanghai
No.65, Yan An Road (West), Shanghai, 200040, China
中国上海市延安西路65号上海国际贵都大饭店办公楼405单元
Phone: +86-21-62489820
Fax: +86-21-62489821

IntechOpen